Effect of Chemical Transport on Stability of Earth Embankment

Ahn, Tae-bong*

요 지

이 연구에서 사용된 화학제는 NaCl이다. NaCl과 모래-벤토나이트 혼합물이 각기 다른 혼합률로 배합되어 삼축 압축 시험을 하였다(5, 10, 15%). 탄성계수와 점착력, 그리고 내부 마찰각이 구속 응력과 NaCl의 함수로 얻었다. 이로부터 구한 강도 정수를 근거로 하여 응력 변형률-강도의 거동 특성을 화학액의 농도함수로 residual flow procedure(REP)에 연결하였다. RFP와 함께 유한요소법을 이용한 사면안정 해석 프로그램을 개발하여 안전율을 구하였으며 강도정수를 화학용액의 농도함수로 요소방정식에 넣어구한 안전율을 비교하였다. 이로써 화학용액이 흙제방의 안정성에 미치는 영향을 분석하였다.

주요어 : 특수계수, 안정성, 화학 물질, 유한요소법, 농도함수

Abstract

In this study, the chemical fluid considered is sodium chloride sloutions. The concentrations for the sodium chloride solutions are varied from 0 to 20%. A series of laboratory triaxial tests are performed on the cylindrical specimens of sand-bentonite mixture with different (5, 10, 15%) sodium chloride content solutions. Deformation(elastic modulus, E) and strength (cohesion, c′, and angle of friction, ϕ') parameters are obtained from the triaxial tests and they are expressed as functions of confining pressure and sodium chloride solution concentrations.

The stress-strain-strength behavior based on the above strength parameters is introduced to the finite element method with a residual flow procedure (RFP). By integrating a slope stability (limit equilibrium) procedure in the finite element method, factors of safety with time are computed.

Keywords : Hydraulic Conductivity, Stability, Chemical Transport, Residual Flow Procedure, Finite Element Method

* Member, Senior Researcher, Korea Institute of Construction Technology

1. Introduction

Environmental problems are some of the most serious problems in the world these days, and various waste disposals such as solid waste and toxic chemical waste are threatening health and even lives of people. When chemicals are introduced into the soil, they affect soil properties such as hydraulic conductivity and stress-strain behavior. Most previous studies have dealt with the hydraulic conductivity of the landfill clay liner; only a few have dealt with stress-strain behavior.

When chemical fluid wastes are disposed in soils, among the main concerns are the location of the extent of chemical fluid and the effect they have on the stability of the structure owing to the changes in soil properties.

The objective of this research is to develop a method to incorporate the effects of chemical transport through soils into soil seepage, stress-deformation, and stability of soil slopes. Development of a procedure to predict chemical influence on seepage and slope stability is essential for further applications in geoenvironmental engineering. Such a knowledge is necessary in order to effectively design and predict the behavior of structures that are affected by migration of wastes.

A powerful procedure called Residual Flow Procedure(RFP) has been developed(Desai, 1976), and applied for combined seepage and stability analysis(Desai and Li, 1983 : Li and Desai, 1983). However, general modeling techniques and methods to incorporate the effects of chemicals on stress-strain-strength behavior have not yet been developed. Moreover, the slope stability analysis of contaminated soil embankments remains largely unattempted. The interface is very important because it indicates the boundary of the contaminated zone. Determination of the location of the interface allows separation of the zone in which the chemical has permeated and the fresh water zone that remains essentially intact.

In this study, the RFP is modified to incorporate appropriate material properties and to perform stability analyses of typical dam problems. The primary scopes of the proposed research are as follows :

(1) Develop a finite element computer program for slope stability analysis that includes the effect of friction angle, cohesion, and modulus for chemically contaminated soil as a function of concentration.

(2) Compare traditional factor of safety and modified factor of safety for chemically contaminated soil slope.

(3) Incorporate factors of safety for stability with time during embankment and during rise or drawdown in reservoir level.

(4) Apply the procedure for solution of various concentration of chemical seepage and stress, and stability analysis.

(5) Develop guidelines for incorporation of effects of other chemicals on soil properties and stability of geotechnical structures.

2. Literature Review

Begining with the research by Anderson et al. (1985) and Madsen and Mitchell (1987), a number of analyses have been carried out to understand the mechanism of the effect of chemicals on soils. These analyses indicate that most chemicals increase the hydraulic conductivity of the soil. In addition to hydraulic conductivity, previous studies have also considered the shear strength properties of sand bentonite mixtures or clayey soils saturated with various chemical fluids. The results have shown that, although the strength of the resulting materials did not have a regular trend, they exhibited changes in undrained shear strength, depending on the chemicals (Evans and Fang, 1988). The shear strength increased with increasing concentrations of leachate for short curing periods, and decreased with longer curing periods (Kenney, 1992). This behavior is explained by possible changes in the clay structure, first to a flocculated, and then to a dispersed matrix with increased duration of interaction of the clay and the leachate. It shows that in addition to hydraulic conductivity, the strength and stress-strain behavior of clay liners are also influenced by interaction between clay and chemical compounds (Kenney, 1992).

3. Details of Theory

3.1 Residual Flow Procedure

In the conventional finite element technique, the unknown a priori flow domain is first approximated by a fixed domain using a variable domain mesh procedure. Variable domain mesh procedure requires finite element mesh for the saturated domain below the free surface to be modified through iterative procedures. However, residual flow procedure (RFP) involves an invariant mesh for the entire domain containing both saturated and unsaturated zones. In the RFP, the governing equations are first assumed to be valid for the entire domain which is treated as saturated. During the iterative solutions separation of saturated and unsaturated zones with different hydraulic conductivities leads to the residual load vector.

Since the entire domain is not saturated, the computed results have error, and they are now corrected by using the residual load vector caused by the effect of the unsaturated zone. RFP involves invariant mesh and avoids mesh modifications and accommodates variable material properties, whereas variable mesh schmes can involve considerable difficulties. Some of the attributes and advantages of the RFP are as follows :

(1) It involves invariant mesh which avoids the need for mesh modifications.
(2) It permits the use of the arbitrary shape of isometric elements, whereas the inequality methods face difficulty in implementing such shapes.
(3) It can accommodate variable properties more easily than the variable mesh schemes.
(4) It can incorporate partially saturated zones.
(5) It is relatively economical in comparison with the variable inequality methods.

The description of RFP dam section shown in Figure 1 is comprised of two zones. One is a fully saturated zone R of the flow domain and the other is a dry or partially saturated zone of 'noflow' domain located above the fully saturated zone. The free surface is the boundary between positive and negative pressures. The governing equation can be written as

$$div(kgrad\phi)+Q=S\frac{\partial\phi}{\partial t} \tag{1}$$

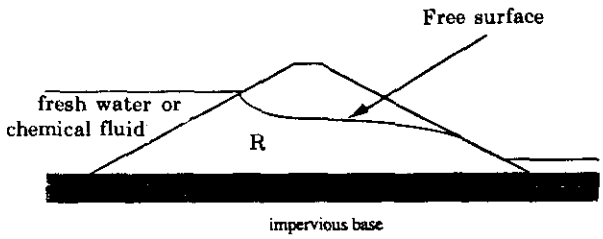

Fig. 1 Schematic Diagram of Unconfined Flow

where k is the hydraulic conductivity of the earth bank, ϕ is the fluid head, and $\phi=z+p/\gamma$. Here, z is the elevation head, and p/γ is the pressure head, S is the specific storage and Q is the applied source or sink. Equation (1) is assumed to hold in both the saturated and unsaturaed domains by introducing a definition of k as

$$k(p) = \begin{cases} k_s \text{ in R} \\ k_s - f(p) \quad \text{elsewhere} \end{cases} \tag{2}$$

where k is the hydraulic conductivity, k_s is the hydraulic conductivity in the saturated zone and $f(p)$ is a function of pressure head.

The element equations are obtained from the stationary condition of a variational function as

$$[k_s]-\{q\}-\{k_{us}\}\{q\}+[P_s]\{\dot{q}\}-[P_{us}]\{\dot{q}\} = \{Q(t)\} \tag{3}$$

where $[k_s]$ is the element hydraulic conductivity matrix for saturated elements, $[k_{us}]$ is the element hydraulic conductivity matrix for unsaturated elements, $[P_s]$ is the element porosity matrix for saturated elements : $[P_{us}]$ is the element porosity matrix for unsaturated elements, {q} is the vector of nodal fluid heads, {Q} is the vector of nodal forcing function, e.g. fluid fluxes, and the overdot denotes derivative with respect to time.

The matrix differential equation is integrated in time by using a finite difference scheme. The fluid head is assumed to vary linearly over a time interval $[t+\Delta t]$ as

$$q(\tau) = q(t) + \frac{\tau - t}{\Delta t}[q(t+\Delta t) - q(t)] \tag{4}$$

where $t \leq \tau \leq t+\Delta t$ and Δt is the time increment. With the scheme in Equation (4), the element equations become

$$([k_s]+\frac{1}{\Delta t}[P_s])\{q\}_{t+\Delta t} = \{Q\}_{t+\Delta t}+[k_{us}]\{q\}_{t+\Delta t}$$
$$+\frac{1}{\Delta t}[P_s]\{q\}_t+\frac{1}{\Delta t}[P_{us}](\{q\}_{t+\Delta t}-\{q\}_t)=\{Q\}_{t+\Delta t}+\{R\} \tag{5}$$

Here, $\{R\}$ is referred to as the residual flow vector.

The residual flow vector $\{R\}$ is evaluated by using the pressure-hydraulic conductivity relation shown in Figure 2(a). For convenience, a simplified form is shown in Figure 2(b), which has been found suitable for most soil problems (Li and Desai, 1983).

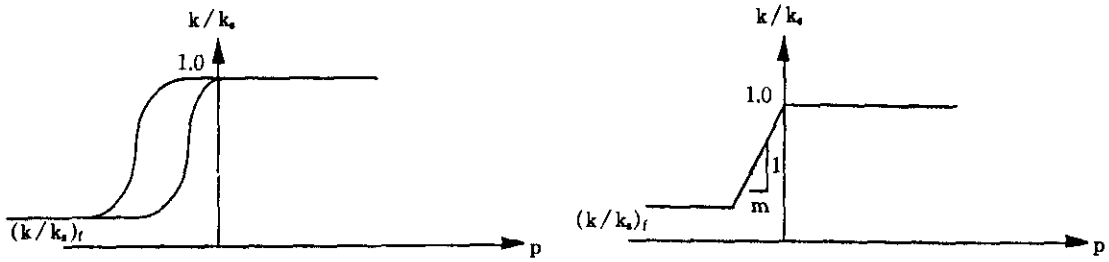

(a) Pressure-Conductivity Curves (b) Idealized Pressure-Conductivity Curves

Fig. 2 The Relationship between Pressure and Hydraulic Conductivity

3.2 Modification of Residual Flow Procedure for Chemical Flow Analysis

Compacted soils are used primarily for the construction of earth embankments and for landfill clay liner in general. These soils are partially saturated during the construction stage ; subsequently, the degree of saturation is increased either by infiltration or by the addition of superimposed loads, and the soil properties may change considerably.

The chemical fluid flow problem which is a typical seepage problem where instead of fresh water chemical fluid is permeant. Usually, the convective dispersion equation is solved for the mass transport problem. However, the RFP is utilized to avoid coupled solutions of the seepage equation and the convective-dispersion equation. Figure 3 is exaggerated in order to describe the free surfaces more clearly. The domain R_1 as shown in Figure 3, is fully saturated and it is a positive pore water pressure zone as utilized for fresh water.

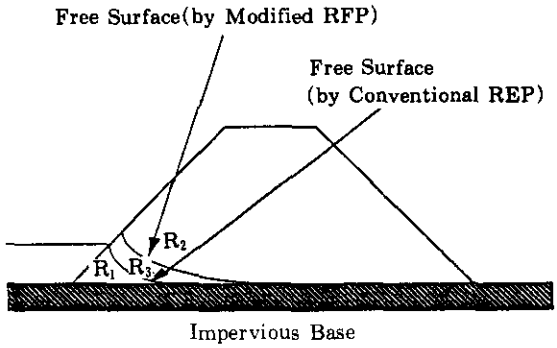

Fig. 3 Schematic Drawing of Chemical Fluid Flow

However, if the upstream fluid is not fresh water, in addition to R_1, a chemically affected zone R_3, which is a capillary zone, can exist above the free surface. The zone R_2 is not affected by chemicals. Since chemical fluid affects soil properties, the capillary zone, R_3, needs to be identified.

Terzaghi(1943) illustrated the principle of capillary flow with a simple model consisting of a column of dry sand with its lower end immersed in water. For simplicity, Terzaghi assumed that at any time the water level in the column of sand represented the boundary between a zone of complete capillary saturation and a zone in which the specimen was completely dry. For this assumption, the rate of capillary rise is governed by Darcy's law (Matyas, 1967).

Hydraulic conductivity of soil as a function of capillary pressure can be represented with a good accuracy by a straight line on a log-log plot over a large range of capillary pressures. This was first pointed out by Gardner (1958) who presented the functional relationship between hydraulic conductivity and capillary pressure over the entire range of capillary pressures as

$$k = \frac{a}{b + p_c^n} \tag{6}$$

where, k=hydraulic conductivity, p_c=capillary pressure, n=positive dimensionless constant, and a and b=constants dependent on the units of hydraulic conductivity. Equation (6) represents hydraulic conductivity as a continuous smooth function of capillary pressure and may often closely approximate the actual relationship.

Published data on porous rocks and other materials show that the relationships between hydraulic conductivity and capillary pressure are often not smooth because hydraulic conductivity is invariant with capillary pressure over a finite range beginning with the capil-

lary pressure of zero. Brooks and Corey (1966) have, therefore, represented the relationship as

$$k = k_w \quad \text{for } P_c \leq P_b$$

$$k = k_w \left(\frac{P_b}{P_c}\right) \quad \text{for } P_c > P_b \tag{7}$$

where k_w=hydraulic conductivity when medium is fully saturated, and P_b=bubbling pressure. Other quantities are as previously defined. It is not possible for the pore pressure to be less than 1 atm($-101 KN/m^2$). If the pore pressure falls below this limit, the pore water will caviate and this limit pressure is defined as bubbling pressure. A typical relationship between hydraulic conducivity and capillary pressure is shown in Figure 4 (Laliberte and Corey, 1967).

The domain R_1 is fully saturated and has positive pore water pressure because it is located below the free surface. The domain R_3 has negative pore pressure, but it is considered to be fully saturated according to the justification by Terzaghi(1943) and Brooks and Corey (1966) as shown in Equation (7). Also, the domain R_2 is partially saturated or completely dry. Therefore, the concentration in domain R_4 is considered to be the same as that of domain R_1. The hydraulic conductivity in the certain range in negative pore pressure is shown to be same as the range of positive pore pressure, and then the hydraulic conductivities decrease linearly to approximately 1% of hydraulic conductivites that hold horizontal as shown in Figure 4. Thus, the idealized pressure-conductivity curve which has been used successfully for fresh water as shown in Figure 5(a) can be modified as shown in Figure 5(b).

The capillary pressure range in which hydraulic conductivity starts to decrease is from 10^4 to 10^5 dynes/cm^2, which is 1 to 10 kPa. It is assumed that the concentration in R_1 and R_4 is the same for upstream. Because it is assumed that the soil is fully saturated in the domains R_1 and R_3, soil strength paramenters such as internal friction angle, cohesion, and modulus need to be modified. The hydraulic conductivity of soil in Figure 5(a) is given below(Desai, 1984) :

$$k(p) = \begin{cases} k_s & in\ (p \geq 0) \\ k_s - f(p) & \text{elsewhere} \end{cases} \tag{8}$$

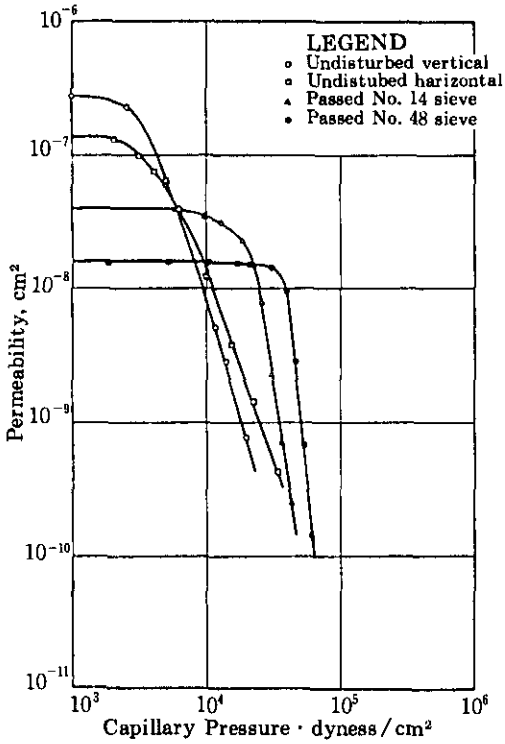

Fig. 4 The Relationship between Capillary Pressure and Hydraulic Conductivity-Fort Colins Clay Loam (Laliberte and Corey, 1967)

where k_s is the hydraulic conductivity of saturated soil with fresh water in the domain R, p is the pore water pressure, and $f(p)$ is a function of hydraulic pressure.

The hydraulic conductivity is now modified into Equation(9) as follows :

$$k(p, c) = \begin{cases} k(c) & \text{for } (p \geq P_a) \text{ in } R_1 \text{ and } R_3 \\ k_s - f(p) & \text{elsewhere}(p < P_a) \text{ in } R_2 \end{cases} \quad (9)$$

where c indicates the concentration of chemicals upstream, P_a is the pressure when hydraulic as shown in starts to decrease, and other variables remain constant. 1 kPa is used for P_a based on Figure 5.

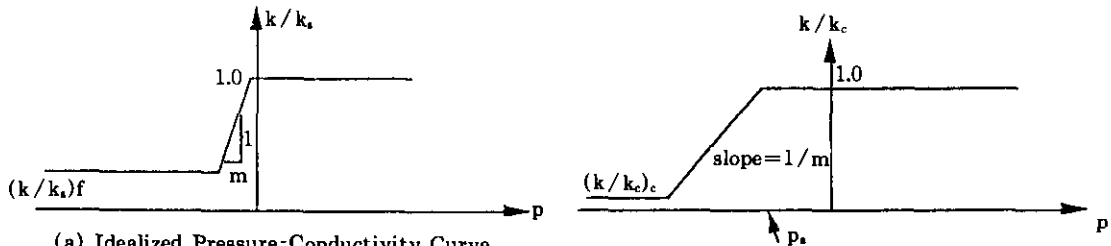

(a) Idealized Pressure-Conductivity Curve of Fresh Water

(b) Idealized Pressure-Conductivity Curve for Chemical Fluid to include Capillary Effects

Fig. 5 Idealized Pressure-Conductivity Curves

3.3 Finite Element Procedure of Stress Analysis

The stress-strain analysis is based on the following incorporation of seepage flow stress analysis as follows. First, the initial stress of the soil mass is computed. Next, by using the residual flow iteration program, the fluid nodal head of the seepage flow is computed. For each element, the centroidal pore pressure is identified. If the pressure is positive, the seepage force and the resultant body force are computed. The change in body force caused by seepage is calculated by the subtraction of the present value from the previously stored value. The incremental nodal forces are then assembled into a global vector and a finite element analysis is performed. The resulting stress and deformations caused by the incremental loading are then added into the existing values. The procdure used here for the finite element analysis is stated as follows :

(1) The element equations for the finite element method procedure used in this work may be expressed as

$$[k]\{q\} = \{Q_e\}+\{Q_s\} = \{Q\} \tag{10}$$

where $[k]$ is the stiffness matrix, $\{q\}$ is the vector of nodal displacements and $\{Q_e\}$ is the vector of the external forces and $\{Q_s\}$ is the vector of the seepage forces, $\{Q\}$ is the vector of external and seepage forces.

(2) The initial stress in the soil mass caused by body forces is computed by solving the following equations :

$$[k]^o\{q\} = \{Q_e\}^o \tag{11}$$

and $$\{Q\}^o = [F]^o\{q\}^o \tag{12}$$

where $\{k\}^o$ is the initial stiffness matrix, $\{q\}$ is the initial deformation vector, $\{Q_e\}^o$ is the initial body force vector, $\{Q\}^o$ is the initial stress vector, and $[F]^o$ is the initial stress-displacement transformation matrix. The superscript o indicates intial conditions.

(3) At each time step, the seepage problem is solved and the seepage forces are found through the computed nodal heads from the seepage analysis at the center of each element. The force is then combined with the gravity force to form a nodal force vector. The following equations are solved in order to obtain the changes in displacements, $\{\Delta q\}^i$, caused by the changes in seepage forces, $\{\Delta Q_s\}^i$:

$$[k]^i\{\Delta q\}^i = \{Q\}^i-\{Q\}^{i-1} = \{\Delta Q_s\}^i \tag{13}$$

where $[k]^i$ is the updated stiffness matrix and
$\{\Delta q\}^i$ is the incremental displacement vector. The stiffness matrix $[k]^i$ is updated to allow nonlinear material behavior.

(4) The seepage force is explained as follows and described in Figure 6.
Consider an element of soil at two diffenrent times. The change in seepage $\{\Delta Q_s\}^i$ between the two times is given by

$$\{\Delta Q_s\} = \{Q_s\}_2 - \{Q_s\}_1 \tag{14}$$

$$\text{where } \{Q_s\}_2 = \begin{Bmatrix} \gamma_d V_{d2} + (\gamma_s - \gamma_w) V_{s2} + Q_{sx2} \\ Q_{sz2} \end{Bmatrix} \tag{15}$$

$$\{Q_s\}_2 = \begin{Bmatrix} \gamma_d V_{d1} + (\gamma_s - \gamma_w) V_{s1} + Q_{sx1} \\ Q_{sz1} \end{Bmatrix} \tag{16}$$

in which γ_d is the unit weight of dry soil, γ_s is the unit weight of saturated soil, V_d is the volume of dry soil, V_s is the volume of saturated soil, and Q_{sx} and Q_{sz} are the components of seepage force vector $\{Q_s\}$ which is evaluated as

$$\{Q_s\} = \iiint_V [B]^T \{p\} dV \tag{17}$$

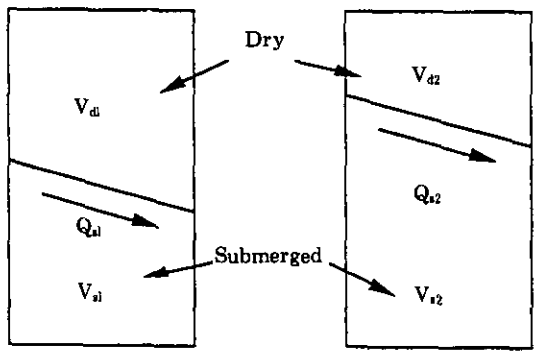

Fig. 6 Schematic Diagram of Soil Element at Two Time Levels

where $\{p\}$ is the vector of fluid pressures.

(5) From the incremental displacement vector, the incremental stress vector is computed and added to the existing stress vector :

$$\{\sigma\}^i = \{\sigma\}^{i-1} + \{\Delta\sigma\}^i \tag{18}$$

where $\{\Delta\sigma\}^i$ and $\{\sigma\}^i$ are the incremental and total stress vectors respectively and $\{\sigma\}^{i-1}$ is the total stress vector of the previous step. Finally, the coordinates of all nodal points are modified according to the incremental nodal displacement, and the stiffness matrix is updated. The procedure is repeated during each time step until the simulation is completed.

4. Experimental Results

4.1 Stress-Strain Curves

The stress-strain curves obtained in the experimental investigation of the samples

saturated with different concentrations of NaCl solution under the various confining pressure are presented in Figure 7 through Figure 9. The experiments were performed by using consolidated-undrained test. The details of the experiment are not described in this paper. It is concluded that the strength of the sand-bentonite mixture increases with the increase in the concentration of NaCl solution. The bentonite used in the mixture is sodium-rich and the NaCl solution is used as the chemical for saturating the mixture. The attraction between the electropositive Na^+ and the negatively charged platelets increases when the mixture comes in contact with the sodium chloride solution. This results in a decrease in the thickness of the diffuse double layer (DDL), leading to a flocculated soil structure and a corresponding increase in the strength.

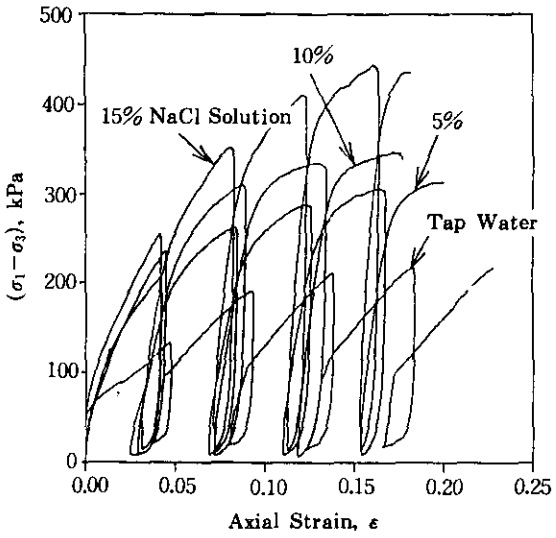

Fig. 7 $(\sigma_1-\sigma_3)$ vs. Axial Strain, ε : σ_3=35kPa

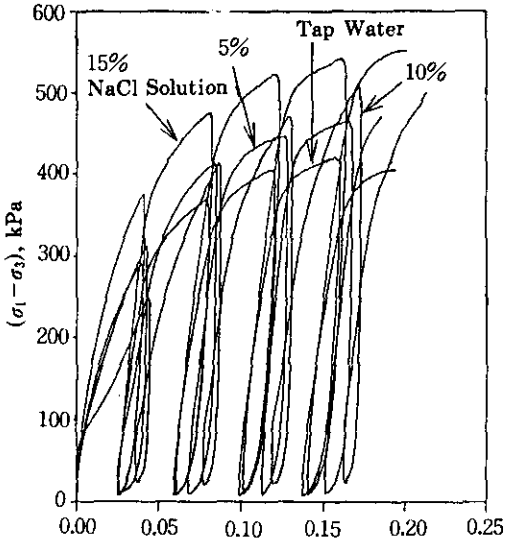

Fig. 8 $(\sigma_1-\sigma_3)$ vs. Axial Strain, ε : σ_3=70kPa

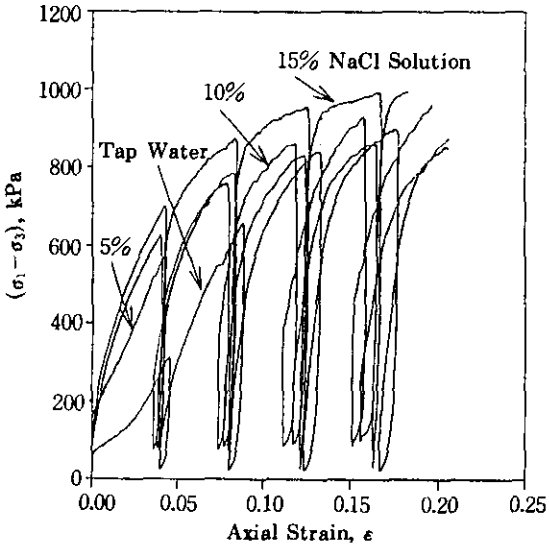

Fig. 9 $(\sigma_1-\sigma_3)$ vs. Axial Strain, ε : σ_3=175kPa

4.2 Variation of Cohesion and Internal Friction Angle

Based on the triaxial tests, it can be stated that effective cohesion, c′, increases as the concentration of the NaCl solution used to saturate the 10% sand-bentonite mixture is increased as shown in Figure 10. As the thickness of the diffuse Double Layer (DDL) decreases, there is a tendency for the soil structure to be flocculated and this reduces the interparticle repulsion. For the combination of sodium bentonite and a saline solution, less fluid is required to neutralize the negatively charged sheets, and if the ion concentration is large, or the valences of the cations are large, the separation distances between sheets will remain small and the montmorillonite particles will remain in the form of closed books.

The effective angle of shearing resistance, ϕ', does not show appreciable change when exposed to different concentrations of NaCl solution as shown in Figure 11. The value obtained is in the range from 44° to 46°.

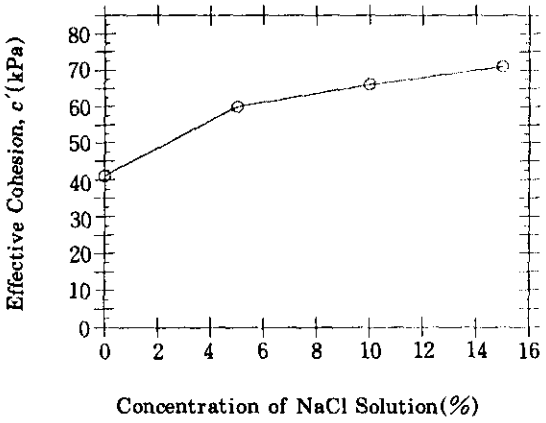

Fig. 10 Effective Cohesion vs Concentration of NaCl Solution

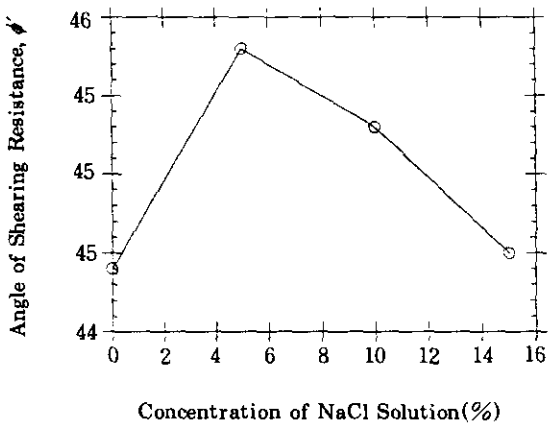

Fig. 11 Angle of Shearing Resistance vs. Concentration of NaCl Solution

5. Safety Factor of Slope Stability

The computer code includes safety factors based on hyperbolic nonlinear elasticity and elasto-plasticty in accordance with the Drucker-Prager material model. These safety factors are calculated from element bases. In the case of the former, the factor of safety for an elements is found from the following.

$$(f \cdot s)_e = \frac{c' + \sigma'_n \tan\phi'}{\tau} \tag{19}$$

where c′ is the cohesive strength, σ'_n is the normal stress, ϕ' is the internal friction angle, τ is the induced shear stress, and the overbar denotes effective quantities. The overall factor

of safety is found as a ratio of the resisting shear strength to the total shear stress along a given slip surface :

$$F.S = \frac{\sum_{i}^{n}(f \cdot s)_i a_i}{L} \tag{20}$$

where a_i is a part of the slip surface intersecting element, L is the total length of the slip surface, and n is the number of elements on the slip surface.

The two soil strength parameters, c′ and ϕ', vary as a function of the concentration of the chemical fluid. The changes of cohesion and internal friction angle influence the factor of safety of the earth dam. When chemical fluid other than fresh water is used as permeant in soils, the soil strength parameters need to be identified through laboratory tests. Since the internal friction angle is constant and the cohesion shows polynomial variation with the concentration of sodium chloride solution verified through cylindrical triaxial tests as shown in Figure 10 and Figure 11, the computer code allows formula for each soil parameter as shown in Equation (21) :

$$\begin{aligned} \phi'(c) &= a \\ c'(c) &= b_1 + b_2 c + b_3 c^2 \end{aligned} \tag{21}$$

where a is constant and, b_1, b_2, and b_3 are the coefficients of second order polynomial functions, and c is the concentration of the chemical fluid. Therefore, Equation(19) is modified as shown in Equation(22) :

$$(f \cdot s)_i = \frac{c'(c) + \sigma'_n \tan\phi'(c)}{\tau} \tag{22}$$

The modified soil parameters are only incorporated below free surface which is calculated from the modified idealized pressure-conductivity relation as shown in Figure 5(b), and remains unchanged from Equation (19) above the free surface. For the intrusion problem, the identical approach could be applied, but modified soil parameters are applied to slope stability analysis for one fluid flow.

By integrating a slope stability procedure in the finite element method with modified soil parameters, factors of safety with time are computed. Overall, the study presents an integrated slope stability and stress-deformation procedure including the effect of chemicals.

6. Examples

In the following problem, a slope stability analysis of a reservoir which holds a chemical

fluid involving transient fluctuation (rise - steady state - draw down) in the upstream head is performed. Various concentrations of sodium chloride as the upstream fluid are compared with an upstream fluid of fresh water. This is not a real case study, but the configuration of the hypothetical homogeneous dam is similar to the Otter Brook dam case studied by another researcher (Li, 1981). Otter Brook dam was constructed in New Hampshire in 1957 with a height of about 39.6m, a base width of 210m and a crest width of about 7.6m. The upstream and downstream slopes have the same slope angle and the geometry of the dam is symmetrical as shown in Figure 12. The finite element mesh uses 112 nodes and 91 elements. The material properties of the hypothetical homogeneous dam that has same dimensions as Otter Brook dam, as used in this analysis, are shown in Table 1 for the increased case. The computer program has plastic model capability. However, same value of modulus is employed for limit equilibrium method and simplicity is shown in Table 1 although different stress-strain behaviors are shown in Figure 7, 8, and 9.

Table 1. Material Properties of Soils in Various Concentrations of Sodium Chloride(Increased Cohesion)

Permeant	Tap Water	5% NaCl	10% NaCl	15% NaCl	20% NaCl
Hydraulic Conductivity(cm/sec)	0.188	0.09	0.09	0.09	0.09
Cohesion(dry)	40kPa	40kPa	40kPa	40kPa	40kPa
Increased Cohesion(wet)*	41kPa	61kPa	67kPa	72kPa	73kPa
Friction Angle (dry)	37	37	37	37	37
Friction Angle(wet)	45	45	45	45	45
Modulus(Dry)	3350kPa	3350kPa	3350kPa	3350kPa	3350kPa
Modulus(wet)	3350kPa	3350kPa	3350kPa	3350kPa	3350kPa
Poisson Ratio	0.38	0.38	0.38	0.38	0.38

* The coefficient b_1, b_2, and b_3 for coehesion are 42.2, 3.7, and 0.1 repectively

* wet means fully saturated and dry means 0% water content. This ideal case is obtained from experiment

The variation of upstream head with respect to time is shown in Figure 13. The upstream head variation is not an actual case, but is idealized to be "rise, steady state, and draw down". Here the upstream level is first allowed to rise steadily and remain in the steady state, then to drop suddenly from an elevation of 30.5m to an elevation of 0.3m above the base of the dam. The draw down rate may not be realistic since in practice a rate of 1m per day would be considered extreme. The high draw down rate is used to dramatize the effects of a sudden draw down. The high rate combined with the relatively high hydraulic conductivity used in the analysis also reduces the simulation time required to produce a noticeable change in the free surfaces.

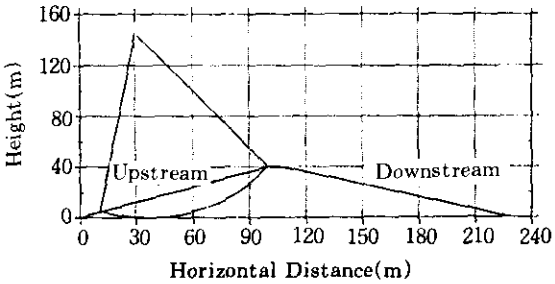

Fig. 12 Diagram of Hypothetical Homogeneous Dam and Failure Surface

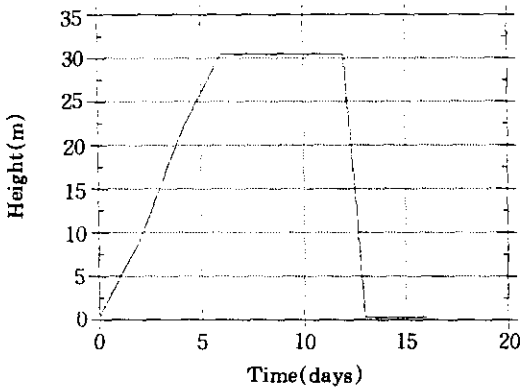

Fig. 13 Upstream Head Variation of Hypothetical Homogeneous Dam over Time

Only cohesion is increased in this hypothetical example because experimental results show increase of cohesion only as shown in Figure 10. The introduction of chemicals that have properties with increasing cohesion as shown in triaxial tests causes a stabilizing effect on earth dam compared with fresh water. The overall safety factor is defined as a ratio of the resisting shear strength to total shear stress along a given failure surface. The normalized overall safety factors over time for fresh water, with 5%, 10%, 15%, and 20% of NaCl are shown in Figure 14. The F_o in Figure 14(b) is the safety factor for the fresh water permeant case at time 0.

The overall safety factors when permeants are sodium chloride solution of various concentrations show similar trend to the case where permeant is fresh water as shown in Figure 14. However, overall safety factors are generally higher than when permeant is fresh

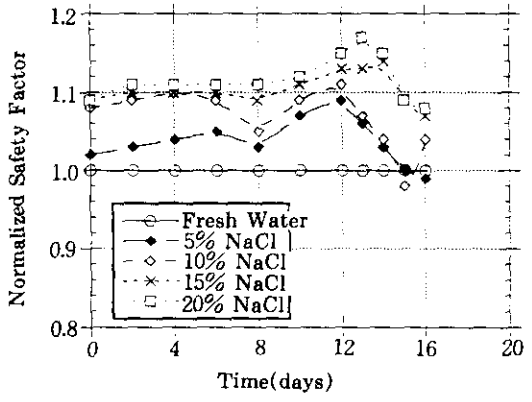

Fig. 14(a) Normalized Overall Safety Factors vs. Time(with respect to Overall Safety Factor of Fresh Water Pemeant at Corresponding Time)

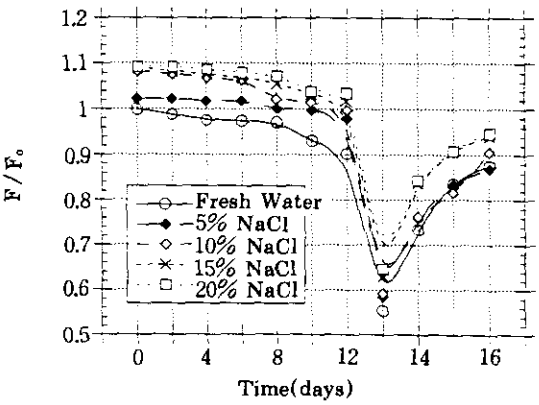

Fig. 14(b) Normalized Overall Safety Factors vs. Time(F_o is Overall Safety Factor of Fresh Water Pemeant at Time 0)

water since NaCl solution increases cohesion of soils.

Overall safety factors decrease slightly during the rise stage. While pore pressure increases during the rise stage, effective stress decreases, and then, the overall safety factor decreases. The overall safety factor decreases by about 30% owing to the build-up of seepage forces during draw down and increases again owing to the dissipation of seepage forces. As concentration increases, the overall safety factor decrease rate is gradually reduced. When upstream head is 0.3m, there is almost no change of overall safety factor because the chemical affected zone almost does not exist. When upstream is completely filled, the chemical effect on stability is the largest.

The overall safety factors over concentration of sodium chloride are shown in Figure 15. The safety factors at the stage of rise, when upstream head is lower(i.e, 0 day), show slower change than higher upstream head(i.e, 12 day) from 0 to 5% of concentration. The increase rate of overall safety factor is high from 0 to 5% of concentration. Then, the increase rate is small after 10%. The overall safety factors after draw down(i.e., 13 day) are less than two for 0 to 20% concentration. The overall safety factor after 14 days shows rapid recovery as shown in Figure 15.

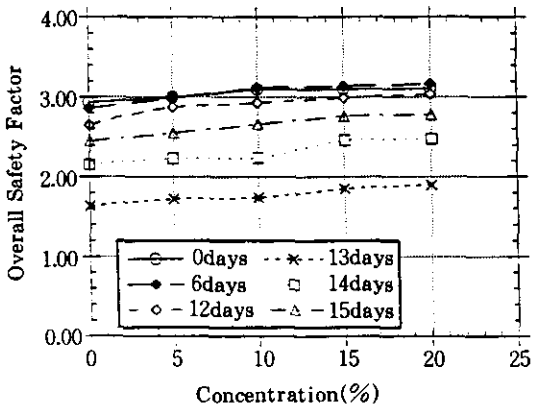

Fig. 15 Overall Safety Factors vs. NaCl Concentrations with Various Time Steps

7. Conclusions

A finite element procedure is developed for stability analysis by including the consideration of friction angle, cohesion, and Young's modulus for chemically contaminated soil to identify effects of contamination on stability. Overall, the study presents an integrated procedure in which constitutive response as affected by salt water is introduced in a finite element procedure. The methodology can permit stress-deformation and stability analyses of geotechnical structures once the stress-strain models, including the effect of chemicals, are established through appropriate laboratory tests.

References

1. Anderson, D. C., Crawley, W., and Zabcik, J. D., (1985), "Effects of Various Liquids on Clay Soil : Bentonite Slurry Mixtures", *Hydraulic Barriers in Soil and Rock.* ASTM STP 874. Philadelphia, pp. 93~103.
2. Brooks, R. H. and Corey, A. T., (1966), "Properties of Porous Media Affectin Fluid Flow" *Irrigation and Drainage Division Journal, ASCE*, Vol 92, No. IR-2.
3. Desai, C. S.,(1984), "Free Surface Flow Through Porous Media Using a Residual Flow Procedure", *Finite Element in Fluid*, Vol.5., Chapter 18, John Wiley & Sons Limited, New York.
4. Desai, C. S., and Li, G. C.(1983), "A Residual Flow Procedure and Application for Free Surface Flow in Porous Media", *Adv. in Water Resources*, Vol. 6, pp.27~35.
5. Desai, C. S.,(1976), "Finite Element Residual Scheme for Unconfind Flow", *Int. Journal. Num. Mech. Engineering.*, 10, pp. 1415~1418.
6. Desai, C. S.,(1972), "Seepage Analysis of Earth Banks under Drawdown" *Journal. Soil Mech. and Found. Div.*, ASCE, Vol. 98, No. SM11, pp. 1143~1162.
7. Evans, J.C., and Fang, H.Y.(1988), "Triaxial Permeability and Strength Testing of Contaminated Soils", *Advanced Triaxial Testing of Soil and Rock*, ed. R. T. Donghe, R.C, and M.L. Silver, ASTM STP 977, pp. 307~404.
8. Gardner, W.R.(1958), "Some Steady State Solutions of the Unsaturated Moisture Flow Equation with Application to Evaporation from a Water Table", *Soil Science*, Vol. 85, April, pp. 229.
9. Kenney et al.,(1992), "Hydraulic Conductivity of Compacted Bentonite-Sand mixtures", *Canadian Geotechnical Journal*, Vol.29, No.3, pp.364~374.
10. Laliberte, G. E., and Corey, A. T., (1967), "Hydraulic Properties of Disturbed and Undisturbed Soils", *Permeability and Capillary of Soils*, ASTM STP 417, pp. 56~65.
11. Li, G. C., and Desai, C.S., (1983), "Stress and Seepage Analysis of Earth Dam", *Journal of Geotechnical Engineering*, ASCE. Vol. 112, No. 6, pp.946~960.
12. Madsen, F.T., and Mitchell, J.K.,(1987), "Chemical Effects on Clay Hydraulic Conductivity and Their Determination", *Geotechnical Practice for Waste Disposal*, ASCE Geotechnical Special Publication.
13. Matyas, E.L.,(1967), "Air and Water Permeability of Compacted Soils", *Permeability and Capillarity of Soils*, ASTM STP 417, ASTM pp.160~175.
14. Sugio, S., and Desai, C. S., (1987), "Residual Flow Procedures for Seawater Intrusion in Unconfined Aquifers", *Inter. Journal for Numerical Methods in Eng.*, Vol.24, pp. 1439~1450.

(received on Apr. 23, 1996)